

DIAGNOSTICS OF DEFORMATION AND FRACTURE STAGES ON THE BASIS OF ACOUSTIC EMISSION, OPTICAL MICROSCOPY AND STRAIN GAUGING

¹Sergey PANIN, ²Stepan KHIZHNYAK, ³Oleg BASHKOV, ¹Anton BYAKOV, ¹Igor SHAKIROV, ¹Victor GRENKE, ¹Mikhail POLTARANIN, ¹Pavel LYUBUTIN, ³Dmitriy SHPAK, ¹Mikhail KUZOVLEV and ¹Marina KIRICHENKO

¹Institute of Strength Physics and Materials Science SB RAS, Tomsk, Russia

²Sukhoi Design Bureau, Moscow, Russia

³Komsomolsk-on-Amur State Technical University, Komsomolsk-on-Amur, Russia

From the point of view of carrying out of experimental researches of deformation behaviour of structural materials the method of acoustic emission (AE) is very informative as allows to obtain the information from entire gauge length of a loaded specimen during generation of deformation defects of a microscale level (first of all, dislocations and their ensembles, twins, etc.). At the analysis of plastic deformation and fracture processes the account of deformation processes and their carriers at larger, in comparison with microscale, levels can be realized by use in situ registration methods (for example, television-optical technique or Digital Image Correlation, speckle interferometry, photoelastic coatings method, ultrasonic diagnostics, etc.) is a great of importance, as well. The importance of multilevel consideration of deformation and fracture processes is caused by variety of deformation processes, their interaction and changing of crucial role at various stages of loading. From the position of experimental research the multilevel consideration can be reached only with use of a various kind and an operating principle of sensors.

An important point during experimental estimation of deformations based on construction of displacement vector fields is continuous “in situ” monitoring over area of strain localization. This can be provided due to localization of deformation processes in the specimen cross-section by making a notch. In the present work the joint research results on features of deformation development of structural materials carried out by means of digital image correlation (DIC), hardware-software complex for registration of acoustic emission (AE – microscale level) and strain gauging are presented.

We investigated peculiarities of deformation development at the micro- meso- and macro levels of flat specimens of different structural materials and alloys as well as ones with a notch. Also, specimens of stainless steel with a surface strengthened by ion nitriding method with various time of thermo-chemical treatment have been analyzed. It was supposed that due to cracking of the strengthened layer the cracks acting of as structural notches of various depths will change the character of deformation localization.

I. INFLUENCE OF CRACKING PATTERN ON AE GENERATION OF SUS 3321 STEEL

Experimental technique and materials. Researches were carried out using materials of various types: low-carbon steel (with 0,2% content of carbon), chromium-nickel stainless steel (SUS 3321), deformable aluminium alloy – duralumin (Al2024), titanium alloy Ti-4Al. Material tests were carried out on mechanical testing machine INSTRON-5582 at uniaxial tension with loading rate of 0.5 mm/min. Specimens were manufactured of sheet materials with thickness of 2 mm. Registration of AE signals was realized with the use of laboratory installation on the basis of PC equipped with four-channel high-speed (ADC) board with sampling frequency of 10 MHz and the following data acquisition parameters: amplification factor - 55 dB, frequency range under registration - 50 ÷ 800 kHz. The analysis of fracture mechanisms of the materials was carried out with the use of newly developed parameters being obtained on the basis of the spectral and wavelet analysis of AE signals [1, 2].

At the first stage of data processing the wavelet analysis was applied for more precise determination of the AE sources location. It is known that main complexity in technique of the AE

sources location is connected with lack of stability in the shape and time of rising of AE signals edge. Allocation of a narrow band of wavelet decomposition factors has allowed to increase accuracy in searching for the AE sources location and to reduce number of "rejected" AE signals.

The second scope of the wavelet analysis application is related to its use as the new parameter for AE signals "decoding" and subsequent identification. Our previously obtained data allow to state that the following parameters of a deformation source such as energy of individual deformation event and its size affect the AE signal formation. The size of the individual deformation event is indirectly connected with the radiation frequency and the elastic acoustic wave energy being raised during deformation. In doing so one can conclude that among main criteria but not only ones for unique defining the type of a deformation source and, as consequence, AE source types are energy and frequency parameter of acoustic radiation. The radiation spectrum of the acoustic wave representing AE signals is wide enough. Therefore direct use of the Fourier spectrum is not absolutely correct. On the other hand the Fourier spectrum is good enough for entire and authentic description of harmonic signals only. However, AE signals are a priori stochastic. Therefore application of the spectrum Fourier-analysis for estimating AE signals frequency is not always meaningful. In this concern the wavelet-analysis based on local estimation of a signal spectrum at any moment can be recognized as the most appropriate the for the frequency analysis of AE signals. The latter being registered during the deformation was analyzed with application of wavelet decomposition. On the basis of detailing wavelet factors (coefficients) the identification parameter, so called frequency factor K_f , defining the contribution value of individual frequency spectrum components into the entire AE signal has been calculated. The frequency factor K_f has been calculated under formulas (1, 2):

$$stdFQ_j = \sqrt{\frac{1}{n} \sum_{i=1}^n (x_{ji} - \bar{x}_j)^2} \quad (1)$$

$$Kf = \frac{1}{m} \sum_{j=1}^m stdFQ_j (m+1-j) \quad (2)$$

where $stdFQ_j$ – standard deviation of J -th factor of wavelet decomposition of a AE signal, n – number of samples in a digitized AE signal, m – number of the wavelet decomposition factors.

Results and discussion. For the analysis of deformation mechanisms and their manifestation an experiment was designed aimed on investigation of influence of a brittle surface layer on deformation features of the material under test at various stages. Chromium-nickel steel (SUS 3321) was researched. Specimens in as-supply state as well as subjected to surface nitriding (nitrogen saturation with time exposure of 1 hour) were tested. Nitrides enriched surface layer with increased hardness and thickness of 10 microns was formed during the thermal-chemical treatment. The initial state and surface hardened specimens were tested at uniaxial tension with simultaneous registration of AE signals as well as optical image at various sites of specimen gauge length for revealing and visualizing the moments of cracks formation in the surface hardened layer.

Experiment 1. In this chapter some investigation results of the steel specimen (SUS 3321) in the as-supplied condition are given. Two-parametrical distribution of AE signals in terms of the energy and the frequency factor K_f is presented in fig. 1. It is seen that energy level of the AE signals is in the range of $0.1 \div 80 \text{ mV}^2\text{sec}$, while parameters of frequency factor vary within a range of $2 \div 4$. In doing so, to the most of signals with value of K_f parameter higher than 3 the value of signals energy less than $10 \text{ mV}^2\text{sec}$ corresponds.

Previously performed investigations of deformation behavior of ductile materials such as pure copper, tin, lead and alloys on their basis, made it possible to established that during their active plastic deformation the majority of radiated AE signals has the parameters being varied within the following ranges: the energy of AE signals – non higher than $10 \text{ mV}^2\text{sec}$; K_f parameter higher than 3. At brittle fracture the majority of AE signals should have the following parameters: for signals with energy less than $10 \text{ mV}^2\text{sec}$ the K_f parameter should be less than 3; for signals with

energy higher than $10 \div 20 \text{ mV}^2\text{sec}$ the value of K_f parameter usually belongs to the range of $2.5 \div 3.5$. The AE signal parameters for brittle fracture were obtained under testing of the quenched carbon steel, tungsten, molybdenum. Thus, based on results of analysis by two-parametrical distribution of any experiment it is possible to distinguish two types of AE signals: being radiated during plastic deformation (under dislocation motion) and during microcracks nucleation and propagation.

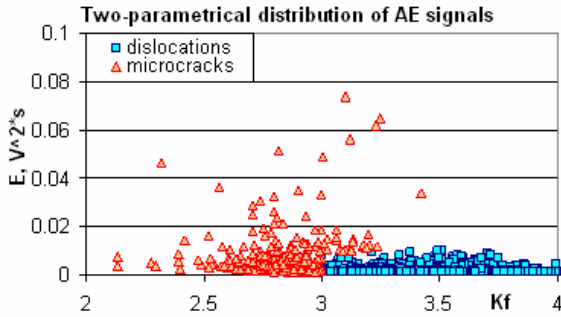


Fig. 1. Two-parametrical distribution of AE signals relative to energy and frequency coefficient under deformation of steel specimen (SUS 3321) at as-supply state.

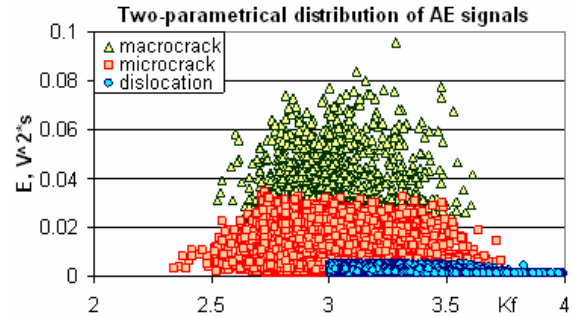


Fig. 3. Two-parametrical distribution of AE signals relative to energy and frequency coefficient (at deformation of steel specimen (SUS 3321) after surface nitriding).

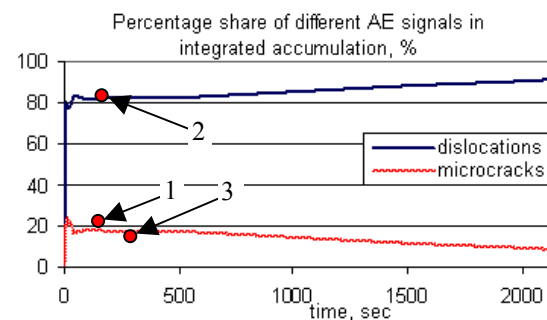
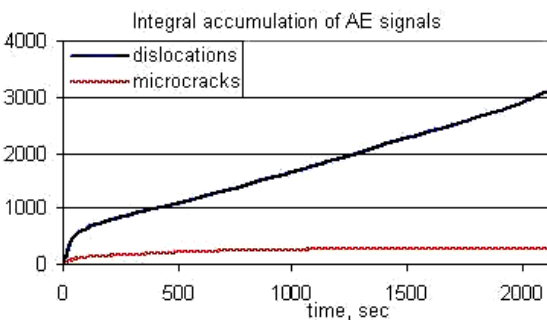
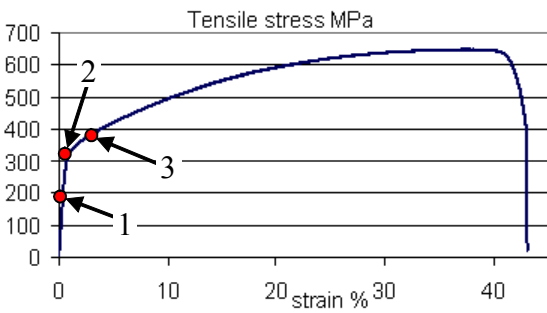


Fig. 2. The loading diagrams and AE parameters under tension of steel specimen (SUS 3321) at as-supplied state.

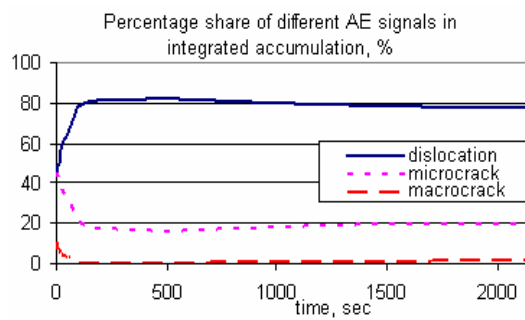
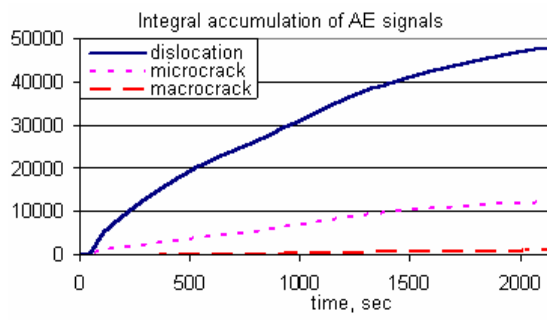
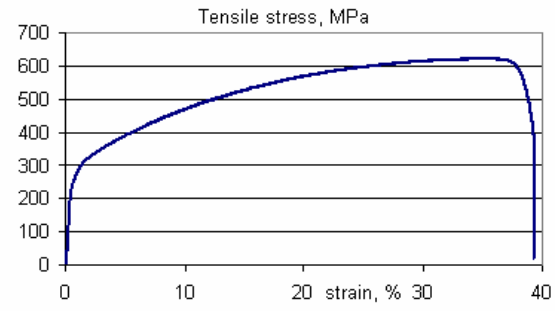


Fig. 4. Loading diagram and AE parameters at deformation of steel specimen (SUS 3321) after surface nitriding

The moments when emission of the signals of both types experiences increase under loading of the steel specimens (SUS 3321) can be illustrated by the diagrams in fig. 2. The latter illustrates: a) the loading diagram and parameters of AE signals accumulation; b) integrated accumulation of AE signals; c) percentage of accumulation in time for both types of the AE signals. As the diagrams show the registration of AE signals unambiguously confirms manifestation of plastic deformation mechanism at the stages of active plastic flow, hardening and fracture. It is seen from fig. 1 that formation of microcracks occurs already at the initial stage.

The further deformation is accompanied by local plastic shears related to dislocation mechanism of plastic deformation. Final fracture (rupture) of the material follows ductile pattern and the forming macrodefect in the form of a neck results from intensive plastic deformation that includes dislocation mechanism. The loading diagram and AE parameters registered during deformation of the steel (SUS 3321) are shown in Fig. 2. Diagrams of AE signal accumulation demonstrate the presence of two types the acoustic signals corresponding the dislocation mechanism and brittle fracture accompanied by microcracks formation. The latter (the given mechanism also can be named as breaking of interatomic bond at microscale level) tends to actively manifest itself at initial deformation stage, i.e. is at elastic deformation. At the given stage only micro-deformations in local volumes occur and most of them results from microcrack formation that become visible from the diagram on fig. 2 (c). This diagram shows the tendency in changing the AE signal percentage which has been accumulated under the action of two various deformation mechanisms. Change of the diagram towards increase in the percentage illustrates the activity growth of the given type of signals in comparison with other type of AE signals, and vice versa. The point 1 in fig. 2 shows the peak of the activity, while point 3 – the beginning of decay of activity of AE sources being identified as the microcracks. The deformation stage designated by the point 2 corresponds to maximal activity of AE sources at the moment when physical yield point of the material is achieved. The AE signals registered at this stage are characterized as ones being radiated at the expense of active movement and generation of dislocations. The subsequent moment of the activity onset for the given type of AE signals corresponds to the point 3. In doing so, the growth of the radiation activity of the dislocation type signals does not stop up to the fracture of the material. Because of the high ductility of the material (elongation at fracture made 43%) even the last stage of main crack formation and fracture is associated with active plastic deformation in the tip of the formed crack that is proved by registered type of the AE signals and viscous pattern of fracture observed in this area.

Fig. 5,a illustrates dependence of shear strain intensity γ as function of loading time for the specimen in as-supply condition. It is seen that starting from elastic loading and up to $\varepsilon \approx 8\%$ the value of γ reaches some constant value and keep it up to fracture of the specimen.

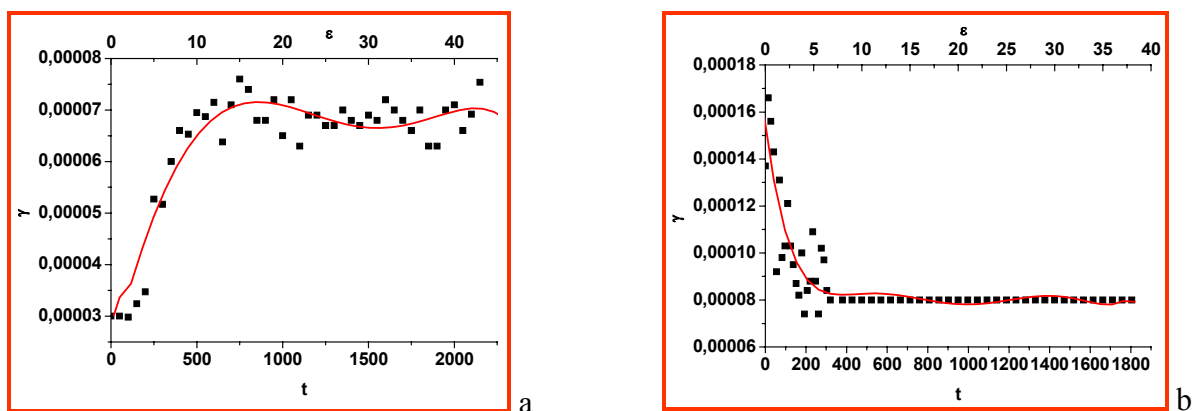


Fig. 5. Integral normalized value of shear strain intensity in initial state (a) and surface hardened (b) specimens as function of loading time.

Experiment 2. In the next experiment tensile tests of steel specimen (SUS 3321) after surface nitriding during one hour was tested. High strength of the surface layer with hardness of 10 GPa and

thickness of up to 10 μm resulted from formation of chromium nitrides Cr_2N there. Two-parametrical distribution of AE signals for the specimen with the nitrated surface layer is presented in fig. 3. One can observe three types of radiated AE signals at the distribution being radiated on account of: i) generation and movement of dislocations, ii) nucleation of microcracks, and iii) initiation of macrocracks. In this case by the nucleation of the microcracks we mean the mechanisms to occur at the microlevel and which are described by the break of interatomic bond groups with low energy and volume where the fracture process takes place. The macrocracks in the given context are the fracture events to occur in local areas comparable with microstructure elements (grains, inclusions, etc.) which can be registered with application of optical observation (microscopy) methods. The total activity of AE signals under deformation of material with two-phase or composite structure is, as a rule rather high. It is related to distinction of mechanical properties of the phases to compose the material. In this case the presence of a ductile phase constrains the process of the material fracture and provides the plastic deformation to develop by a slightly different mechanism in contrast with a material without a surface hardened layer. Even at elastic deformation stage the increase of stresses in places of their greatest concentration in surface layers takes place. The given process results in nucleation of the microcrack grid distributed over entire surface of the strengthened material. It is confirmed by the diagram in fig. 4 (b) – at an initial stage of loading (point 1) one can observe similar amount of two types of the AE signals: radiated from i) dislocation and ii) nucleation of microcracks. At the same stage there are also distinguished first macrocracks to form in the surface layer that is proved by registration of corresponding type of the AE signals. Further activity in radiation of the AE signals from nucleated micro- and macrocracks decreases in relation to the initiation of plastic deformation in substrate zones adjacent to the cracks in the surface hardened layer (point 2 and 3). One can observe the activity of plastic deformation in these regions by formation of mesobands of localized plastic shears spreading from crack tips at the angle of 45° to the loading axis. Active growth of the dislocation type of the AE signals (point 4) is observed at this stage. The further deformation develops without essential change of the activity of both mechanisms. However, when strain degree achieves 10% the monotonous decrease of the percentage of the dislocation type AE signals takes place while corresponding increase of the AE signals identified as the formation of micro- and macrocracks starts. This is related to damage accumulation to be formed mostly due to propagation of new defects inside the substrate whose origin corresponds to the macrocracks in the surface hardened layer.

Fig. 5,b illustrates dependence of shear strain intensity γ as function of loading time for the specimen with surface hardened layer. One can easily see from the figure that at beginning of loading the value of γ has very high values that is related to nucleation of large through cracks and strain localization in the substrate. Just after the primary cracking process is stopped γ oscillates within nearly constant value equal to 0.0008. The latter means that deformation development in the specimen is governed mostly by quasi-uniform plastic deformation development in the ductile substrate.

In the way of summarizing it should be noticed that in this part of the paper we researched deformation development pattern of steel specimens (SUS 3321) in the as-supplied state as well as with surface hardened layer obtained by gas nitriding. On the basis of previously obtained data (under deformation of a wide range of materials) the technique for classification of AE signals with the aim of identification their sources has been developed. For a number of materials the three types of AE signals have been distinguished: i) the signals radiated at movement of dislocations (the dislocation mechanism) and the signals radiated at formation of ii) micro- and iii) macrocracks. The results of the AE signals analysis for investigated steel (SUS 3321) has shown the following:

- Stage pattern of material deformation process: the stages of microplasticity, yielding, hardening, cracking;
- Stage pattern of deformation development at the micro- and mesolevels for both types of specimens: with homogeneous structure and two-phase macrostructure (surface-hardened layer-substrate);

- At the stage of elastic deformation the microplasticity and microcracking mechanisms are prevailed;
- Nucleation of the main crack and fracture of a ductile material develops with intensive plastic deformation in the crack tip.

The further prospects of the given research are oriented towards improving the technique of AE signal decoding and constructing structure-sensitive model of the AE signals with the aim of deformation and fracture process identification.

II. INFLUENCE OF NOTCH CONFIGURATION ON STAGE PATTERN OF AA2024 SPECIMEN DEFORMATION

Materials and investigation technique. Aluminum alloy AA2024-T4 specimens in the as-received condition were tested. Three semicircular notches of 300 μm depth being located different distances from each other were applied according to the scheme shown in fig. 6.

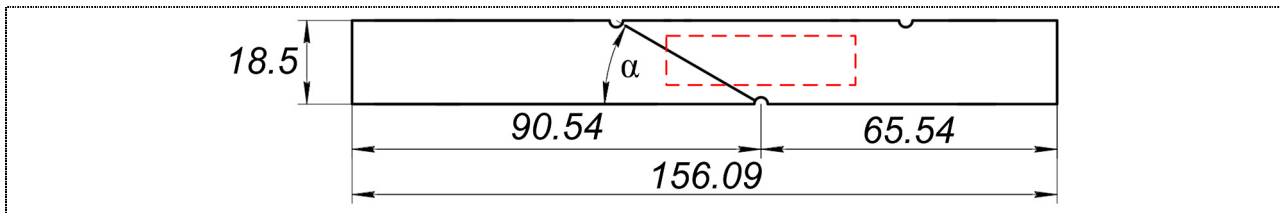


Fig. 6. Scheme of the notches application (a) and optical images of the specimens. Angle between notches makes: b) $\alpha=30^\circ$; c) $\alpha=45^\circ$; d) $\alpha=60^\circ$; e) $\alpha=70^\circ$

Uniaxial tensile tests were performed at electro-mechanical testing machine Instron 5582 with the loading rate of 0.3 mm/min. Surface micrographs were recorded by means of SLR digital camera Canon EOS 350 equipped with telephoto lens CarlZeiss Jenna Sonnar 300/4. The size of the specimen observation area for mapping displacement vectors and subsequent calculation of shear strain intensity (by means of Television Optical Meter for Surface Characterization - TOMSC) were physical size – 18.5×90 mm; the resolution of digitized image – 750×3450 pixels. For the calculation of the average value of shear strain intensity γ_{norm} , the area with the size 328×1230 pixels (physical size 8×32 mm) located in the center between stress concentrators (indicated by a red frame in fig. 6, a) was chosen.

Microscale level. Analysis of AE registration data. Dependences of AE event counting rate versus time of loading $\partial N_{\text{AE}}/\partial t$ for specimens of all type are depicted in fig. 7. This parameter was chosen for the analysis as being the most "sensitive" to the change of the leading (key) scale level of deformation in a specimen under loading. The curves were fitted by polynomial approximation of degree 6 (fig. 7). The analysis of the obtained results as well as the data in fig. 7 showed that the number of registered AE events for specimens under tests both of identical shape and with different angles between notches was not constant; therefore the integrated number of AE events is not discussed in the paper as a comparative parameter.

Mesoscale level. Shear strain intensity – integral analysis. The analysis of strain evolution at the mesoscale level was made by means of processing images by the integral and differential method. In the first case displacement vectors were mapped by comparison of a first (initial) image with each subsequent one, while in the differential way of calculation a current and a subsequent images of a deformed specimen surface were compared. Dependences of average values of the shear strain intensity ($\gamma_{\text{norms int}}$) obtained from the analysis of images by the integral method are the principal in fig. 8. It should be noted that rather small values of the calculated deformations are related to use of the smoothing procedure (vectors filtration) for the reduction of the influence of incorrectly constructed vectors on local strain values.

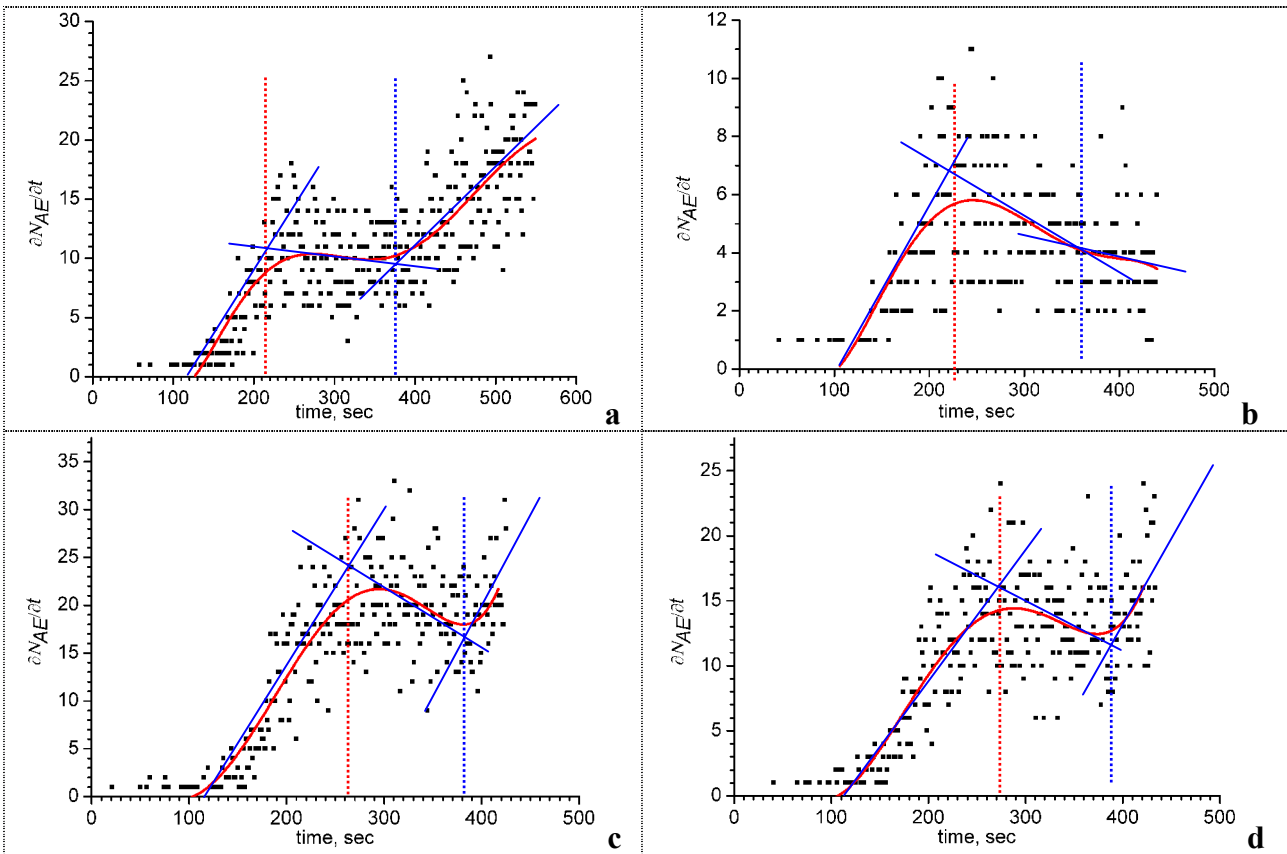


Fig. 7. Dependences of AE event counting rate versus time of loading $\partial N_{AE}/\partial t$. Angle between notches makes: a) $\alpha=30^\circ$; b) $\alpha=45^\circ$; c) $\alpha=60^\circ$; d) $\alpha=70^\circ$

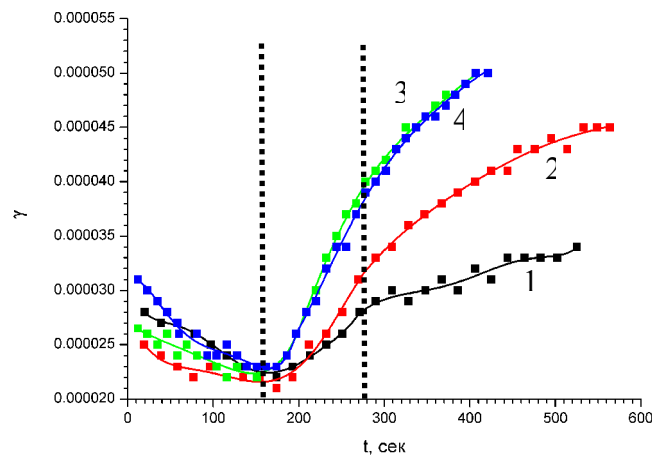


Fig. 8. Dependences of the shear strain intensity versus loading time for AA2024-T4 specimens calculated by the integral method: a) $\alpha=30^\circ$; b) $\alpha=45^\circ$; c) $\alpha=60^\circ$; d) $\alpha=70^\circ$.

The results testify that in the specimen with $\alpha=30^\circ$, where the notches are located at a significant distance from each other, consequently they do not exert mutual influence on the character of the deformation macro-localization. The sample with $\alpha=45^\circ$ takes an intermediate position in which orientation of the localized deformation macro-bands coincides with direction of the maximal shear stress. The maximal rate of $\gamma_{norms\ int}$ change is typical for specimens with angles between notches of $\alpha=60^\circ$ and $\alpha=70^\circ$. The reason is associated with the formation of the deformation localization zone of the significant size due to connecting of each pair of notches and including two macro-bands of localized shear. This conclusion was proved by further investigations (see below) by numerical simulation with the use of the ANSYS FE package. This effect was investigated in more detail through use of the differential method of displacement vector mapping.

Shear strain intensity – differential analysis. Dependences of the shear strain intensity calculated by the differential method of the image processing which, undoubtedly, is more sensitive to local strain changes (that is also proved by larger scattering of the specified parameter value shown in fig. 9). This explains the necessity of their sectionally-linear approximation.

Generally, by qualitative observation the dependences shown in fig. 9 can be divided into 2 groups: i) a long second transient stage and decreasing value of $\gamma_{\text{norm dif}}$ at the stage of the strain macro-localization (for the specimens with the angle of $\alpha=30^\circ$); ii) a short transient stage and constant or increasing value of $\gamma_{\text{norm dif}}$ at the macro-localization stage. Thus, in contrast with the diagram for the integral method of $\gamma_{\text{norms int}}$ calculation depicted in fig. 9, for the differential method of $\gamma_{\text{norms dif}}$ calculation, when macro-bands are oriented along the direction of the maximal shear stress ($\alpha=45^\circ$), an increase of normalized values of the shear strain intensity at macro-localization stage (third stage) is observed. At the same time, for the integral method of calculation the maximal growth rate was observed for specimens with an angle between notches of $\alpha=60^\circ$ and $\alpha=70^\circ$.

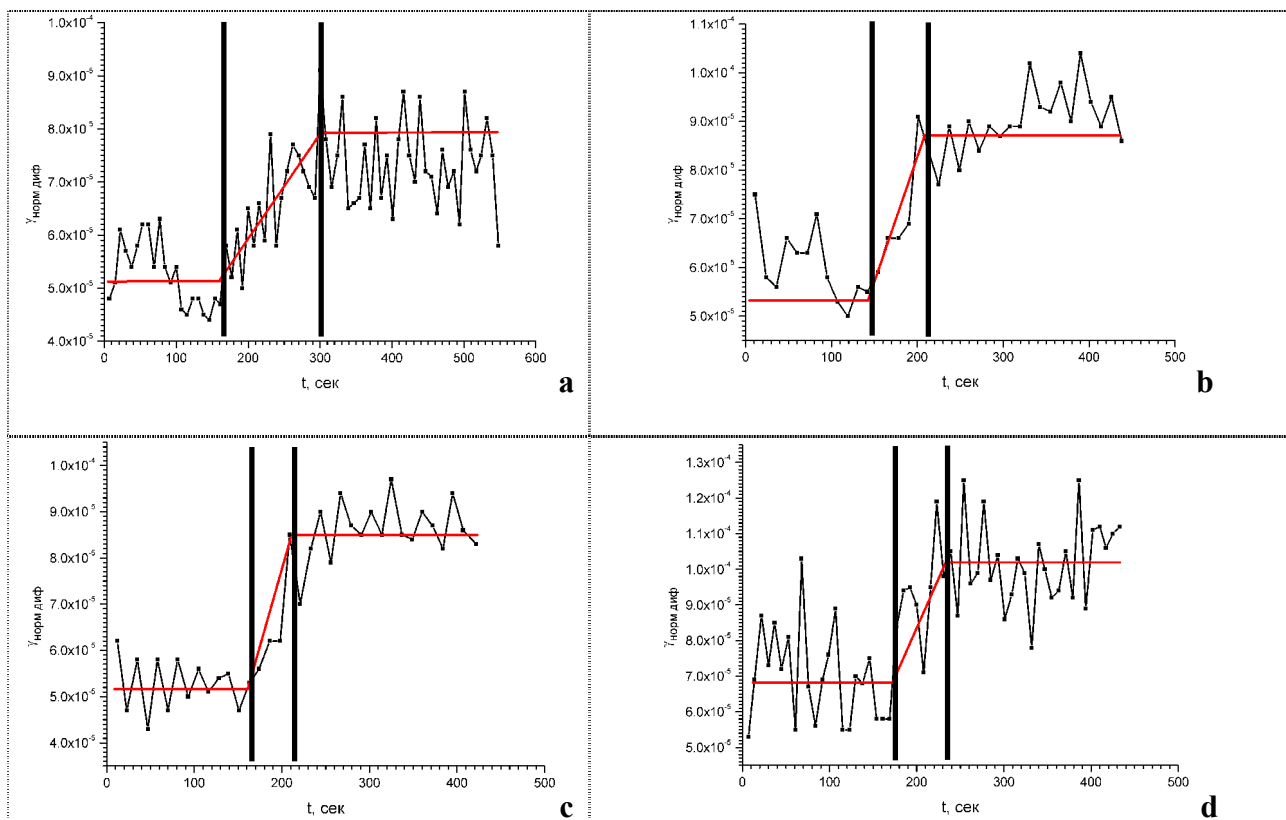


Fig. 9. Dependences of the shear strain intensity on time loading for AA2024-T4 specimens calculated by the differential method ($\gamma_{\text{norm dif}}$) versus loading time. Angle between notches makes: a) $\alpha=30^\circ$; b) $\alpha=45^\circ$; c) $\alpha=60^\circ$; d) $\alpha=70^\circ$

Macroscale level. Calculation by the ANSYS package. The hypothesis discussed in the paper about the influence of the notch location onto change of the deformation localization character also was analyzed by carrying out numerical experiment by engineering software package ANSYS 5.4. Results of the calculation of average stress values for samples of all types are presented in fig. 5. These results show that when the angle between notches makes $\alpha=30^\circ$, the interaction between them is practically absent; increase of the angle up to $\alpha=45^\circ$ causes the formation of two strain macro-bands connecting the next; when the angle makes $\alpha=60^\circ$ and $\alpha=70^\circ$, the macro-localization area is formed of a certain extent containing two macro-bands coming from the opposite direction, extending from each adjacent notches.

It should be noticed that results described in this part of the paper corresponds to stress intensity distribution at elastic loading range and do not correlates exactly with the strain localization

processes. Nevertheless, being considered qualitatively the calculations performed allows us to follow pattern of interaction of the neighboring notches and their mutual influence on stress distribution in the specimen.

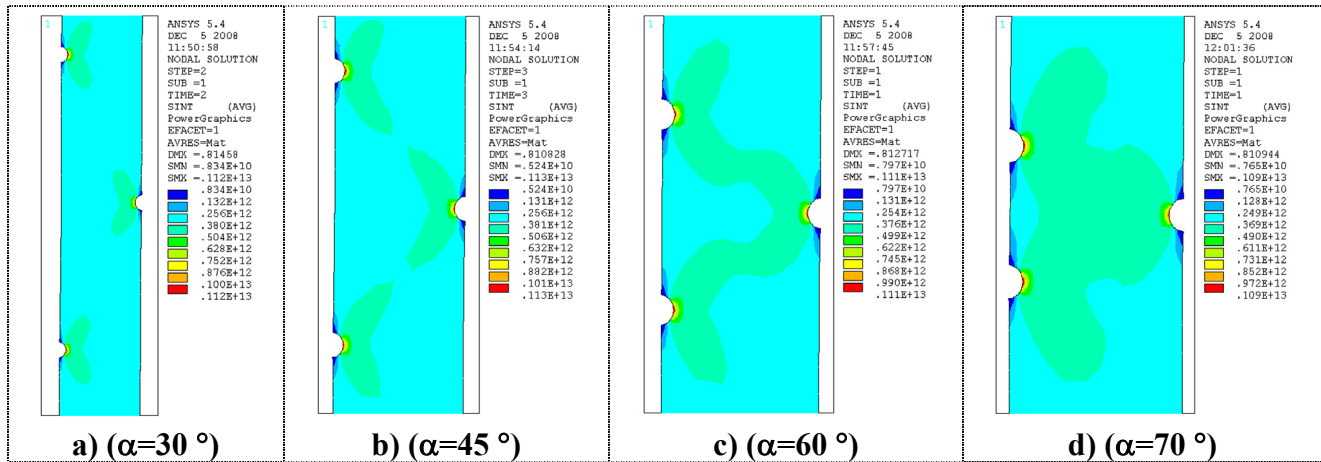


Fig. 10. An example of calculation of the stress intensity made for specimens with different angles between notches (calculation for an elastic range) with use of ANSYS package. Angle between notches is: a) $\alpha=30^\circ$; b) $\alpha=45^\circ$; c) $\alpha=60^\circ$; d) $\alpha=70^\circ$

Macroscale level. Loading diagrams. Fig. 11 illustrates dependences of external load derivative over time as function of loading time and loading diagrams for all specimens under investigation. It should be noticed that all graphs look the same. In particular, for the graph presented on fig. 11 (a) for the specimen with the angle of $\alpha=30^\circ$ one can distinguish two characteristic parts (stages) of $\partial\sigma/\partial t$ value being quite satisfactory fitted by straight lines. On the basis of piecewise-linear approximation as well as similar to above described results we distinguish several characteristic stages of $\partial\sigma/\partial t$ changing. It is of interest that characteristic time corresponding to two turns on the dependence shown at fig. 11 (a) approximately corresponds to ones at fig. 8. This once again confirms sensitivity of technique of shear strain intensity calculation to the change of key level of plastic deformation.

In doing so, the analysis of the processes under consideration in terms of their stage pattern make it possible to reveal correlations between characteristics to describe deformation development at different scale levels.

4. Conclusions

It is shown that deformation localization caused by a notch in a different degree affect the pattern of acoustic emission under deformation of various materials. In more ductile materials (AMG6AM, steel 20) increase in acoustic activity is observed when the specimens have notches. The last, most likely, is related to intensive strain hardening of materials under investigation in the vicinity of the notch. Deformation of notched specimens of materials of less ductility (steel 45, titanium alloys OT4, VT20) is accompanied by reduction of the registered number of AE events at conservation of signals energy during the test. The given result, most likely, is associated with the small area of deformation localization zone and the general reduction of number of moving and formed defects of acoustic emission potential sources.

The use of the combination of DIC and AE data allows examining precisely staged patterns for deformation processes development at various scale levels. At the initial stages of loading the AE method seems to be the most sensitive to deformation processes that allows identifying the transition from the first to the second stage. At greater degrees of deformation the method of digital image correlation (DIC) more precisely characterizes the change of the key role from meso- to macroscopic scale of the deformation development. The analysis of the processes of localized plastic deformation in terms of pattern stages is presented as an effective way of data interpretation concerning the deformation evolution at various scale levels.

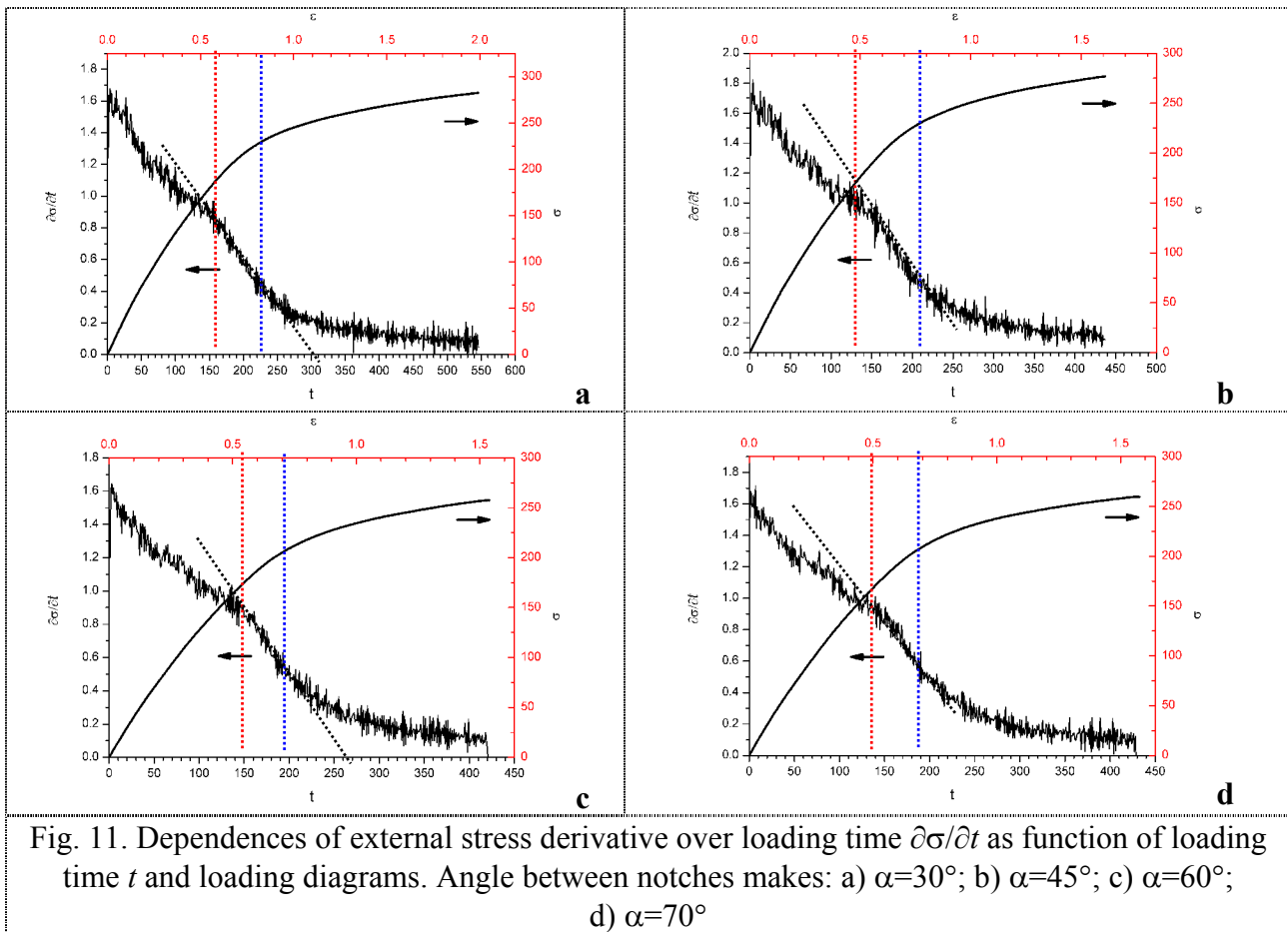


Fig. 11. Dependences of external stress derivative over loading time $\partial\sigma/\partial t$ as function of loading time t and loading diagrams. Angle between notches makes: a) $\alpha=30^\circ$; b) $\alpha=45^\circ$; c) $\alpha=60^\circ$; d) $\alpha=70^\circ$

The researches carried out have revealed the pronounced interrelation between character of AE signals change and intensity of strain development being gained by results of the television-optical measurements and strain gauging. The results obtained are evident acknowledgement of well-manifested interrelation of plastic deformation processes at various scale levels. The calculated numerical values of analyzed parameters have allowed finding the conformity between intensity of AE signals and a degree of deformation localization of deformed specimens, first of all, in terms of stage patterns for the analyzed processes.

References

1. O.V. Bashkov, D.A. Shpak and I.M. Gololobova: Proc. of VIII Russian-Chinese symposium «Modern materials and technologies». Khabarovsk. 2(2007), 83-87.
2. O.V. Bashkov, D.A. Shpak: Joint China-Russia Symposium on Advanced Materials and Processing Technology. Harbin, China, (2008), 365-370.